ACCEPTED BY AJ 2004 FEBRUARY 23
Preprint typeset using LaTeX style emulateapj v. 2/19/04

M/L, Hα ROTATION CURVES, AND H I GAS MEASUREMENTS FOR 329 NEARBY CLUSTER AND FIELD SPIRALS: III. EVOLUTION IN FUNDAMENTAL GALAXY PARAMETERS

NICOLE P. VOGT[1,2]
Department of Astronomy, New Mexico State University, Las Cruces, NM 88003
AND
MARTHA P. HAYNES,[3] RICCARDO GIOVANELLI,[3] AND TERRY HERTER
Center for Radiophysics and Space Research, Cornell University, Ithaca, NY 14853
Accepted by AJ 2004 February 23

ABSTRACT

We have conducted a study of optical and H I properties of spiral galaxies (size, luminosity, Hα flux distribution, circular velocity, H I gas mass) to investigate causes (*e.g.*, nature versus nurture) for variation within the cluster environment. We find H I deficient cluster galaxies to be offset in Fundamental Plane space, with disk scale lengths decreased by a factor of 25%. This may be a relic of early galaxy formation, caused by the disk coalescing out of a smaller, denser halo (*e.g.*, higher concentration index) or by truncation of the hot gas envelope due to the enhanced local density of neighbors, though we cannot completely rule out the effect of the gas stripping process. The spatial extent of Hα flux and the *B*-band radius also decreases, but only in early type spirals, suggesting that gas removal is less efficient within steeper potential wells (or that stripped late type spirals are quickly rendered unrecognizable). We find no significant trend in stellar mass-to-light ratios or circular velocities with H I gas content, morphological type, or clustercentric radius, for star forming spiral galaxies throughout the clusters. These data support the findings of a companion paper that gas stripping promotes a rapid truncation of star formation across the disk, and could be interpreted as weak support for dark matter domination over baryons in the inner regions of spiral galaxies.

Subject headings: galaxies: clusters — galaxies: evolution — galaxies: kinematics and dynamics

1. INTRODUCTION

Recent years have seen the emergence of a standard model for the growth of structure – the hierarchical clustering model – in which the gravitational effects of dark matter drive the evolution of structure from the near-uniform recombination epoch until the present day. Simple models for galaxy formation in the context of these CDM cosmogonies have been remarkably successful in reproducing the properties of the local galaxy population (Kauffmann, White, & Guiderdoni 1993; Cole *et al.* 1994) and have been extended to predict the sizes, surface densities and circular velocities of spiral galaxy disks (Dalcanton, Spergel, & Summers 1997; Mo, Mao, & White 1998).

The result has been a testable scenario that predicts the basic structural properties of the disk galaxy population in any specific cosmogony of CDM type, and how the ensemble of disk galaxies should evolve with redshift. The models assume that most spirals formed as the central galaxies of isolated halos, an assumption supported by the fact that they must have undergone minimal dynamical disturbance since the formation of the bulk of the disk stars (Tóth & Ostriker 1992). The size of the disk is thus expected to scale with that of its halo, and at high redshift the predicted distribution of halo sizes is shifted to smaller values.

By $z = 1$ the predicted change in disk size is almost a factor of 3 for an Einstein-de Sitter Universe, though only about 1.5 for a flat universe with $\Omega_0 = 0.3$. High redshift field spirals show some evidence for this effect (Vogt 2000), though surface brightness selection biases can mimic this trend and it is difficult to separate the two factors (Vogt *et al.* 2004c). Alternatively, one can search for evidence within the fossil record of local clusters. Specifically, spiral galaxies which formed early in the vicinity of rich clusters may preserve signatures of early coalescence (Kauffmann 1995), even as we observe them today. The difficulty, of course, is to distinguish between such cosmological variations in disk structure and in the direct effects of the cluster environment. Some fundamental disk properties (*e.g.*, scale length) may prove to be more a function of the cluster-wide environment than of the galaxy-specific environment, while the properties of the gas reservoir are strongly dependent upon the individual merger history and on interactions with the intracluster medium.

There have been a number of theoretical approaches to modeling the Tully-Fisher (Tully & Fisher 1977) relation and its implications for disk formation and evolution (Rhee 1996; McGaugh 2000; van den Bosch 2000 and references therein). Its successful use to probe the peculiar velocity field about clusters is dependent on the assumption that the relevant galaxy properties do not vary significantly in different environments. Ideally Tully-Fisher studies utilize many galaxies within a cluster to reduce the distance error estimate; by measuring velocity widths from Hα rotation curves, H I selected samples can be augmented with gas-poor galaxies for which the H I line profile cannot furnish a velocity width (*cf.* Giovanelli *et al.* 1997a). This increases the sampling of a cluster, and in addition H I stripped spirals are the most likely to be true cluster members rather than members of infalling groups, offset both on the sky and in projection.

Evidence for systematic changes in the Tully-Fisher rela-

Electronic address: nicole@nmsu.edu
Electronic address: haynes, riccardo, and herter@astro.cornell.edu
[1] Formerly at: Institute of Astronomy, University of Cambridge, Cambridge, CB3–0HA, UK
[2] Formerly at: Center for Radiophysics and Space Research, Cornell University, Ithaca, NY 14853
[3] National Astronomy and Ionosphere Center; NAIC is operated by Cornell University under a cooperative agreement with the National Science Foundation.

tion as a function of environment could invalidate such studies. Variations in the mass and light distribution of galaxies with environment could thus have a significant effect, as the Tully-Fisher relation might vary not only between the field and clusters, but, if environmental effects are important, from cluster to cluster depending upon its evolutionary state. Furthermore, Salucci, Frenck, & Persic (1993) argue that the scatter in the Tully-Fisher relation can be decreased by decomposing the mass distribution within galaxies into a dark and a luminous component to isolate the contribution of the disk alone to the circular velocity of the system (see however Jablonka & Arimoto 1992), implicitly emphasizing the need for detailed knowledge of the environmental variations of the dark and luminous mass distributions. Though most of the Tully-Fisher studies performed to date have not contained large or sufficiently well–defined samples to properly assess environmental impacts, there is some evidence (Biviano *et al.* 1990) against a strong dependence of the Tully-Fisher relation calibration upon mean cluster densities, radial positions of galaxies within clusters, or galaxy morphologies.

There is also evidence that the Tully-Fisher relation and the $D-\sigma$ relation, and other fundamental plane relations, do not necessarily produce the same results when applied in parallel. The peculiar velocities derived by Aaronson *et al.* (1986) for spirals, and by Lucey *et al.* (1991) for ellipticals and S0s, within the cluster A2634, for example, differ significantly. The effects of the cluster environment upon the two populations may be a very relevant factor, as is the evidence for an environmental correlation in the zeropoint of the $D-\sigma$ relation (Lucey *et al.* 1991; Guzmán 1993). However, the effects of infalling group velocities and, in this case, the possible inclusion of galaxies from the very nearby cluster A2666 (Scodeggio *et al.* 1995) must also be examined.

Our program integrates both optical and H I observations; we seek to form a consistent picture of infalling spirals which is sensitive to both gas depletion and star formation suppression. Our sample is made up of 329 galaxies, 296 selected from 18 nearby clusters and 33 isolated field galaxies observed for comparative purposes. It extends over a wide range of environments, covering three orders of magnitude in cluster X-ray luminosity and containing galaxies located throughout the clusters from rich cores out to sparsely populated outer envelopes. We have obtained Hα rotation curves to trace the stellar disk kinematics within the potential at high resolution and to explore the strength of current star formation, H I line profiles to map the overall distribution and strength of H I gas, and *I*-band imaging to study the distribution of light in the underlying, older stellar population. The sample contains spirals of all types, and is unbiased by the strength of flux from H II regions or by H I gas detection. This paper is a companion to Vogt, Haynes, Herter & Giovanelli (2004a, Paper I), which details the observations and reduction of the data set, and to Vogt, Haynes, Giovanelli & Herter (2004b, Paper II) which explores the evidence for spiral galaxy infall.

2. EVOLUTION IN FUNDAMENTAL PARAMETERS

2.1. *Sampling Bias within the Dynamical Sample*

Taken together, these points all serve to motivate our examination of the fundamental parameters for cluster spirals for environmental variations. We proceed to explore the space defined by luminosity, size and circular velocity through the size-velocity relation, the surface brightness diagram, and the Tully-Fisher relation. We first examine three representative variables for bias. The process used is derivative of that for our larger Tully-Fisher program, discussed in great detail within Giovanelli *et al.* 1997ab. We begin by examining the distribution of disk scale length R_d, circular velocity ΔV_{circ}, and *I*-band magnitude $M_I - 5$ log h across the dynamical sample. These data have been corrected for the effects of extinction, inclination, and seeing conditions. We wish to compare the distribution of these fundamental parameters, which differ in their dependence on distance, against each other. We will control out the effect of peculiar velocities for each cluster, by comparison of the standard Tully-Fisher relation (*i.e.* total *I*-band magnitude $M_I - 5$ log h versus terminal circular velocity ΔV_{circ}) offsets with a template relation derived for a large, overlapping distribution of clusters spread around the sky (the "basket of clusters" approach, where the template relation has been derived from clusters at cz $\sim$ 6,000 km s^{-1}, Giovanelli *et al.* 1997b). In order to compute a valid Tully-Fisher relation for each cluster, we must first evaluate the effects of bias in cluster sampling.

Cluster sampling can be biased by a large number of selection effects, including the undersampling of faint galaxies, the homogeneous Malmquist bias (*cf.* Lynden-Bell *et al.* 1988) due to the increase in sampled co-moving volume with distance which scatters distant objects preferentially into the sample, and variations of galaxy properties with morphological or environmental variations. We refer the reader to an extended discussion of the impact of these factors within Dale *et al.* 1999b, arguing the negligible impact of all but the sampling bias towards the bright end of the luminosity function, and the the discussion ahead in Section 2.3.3 confirming the small effects of the cluster environment on the Tully-Fisher relation within the dynamical sample. The effect of the bias towards bright galaxies, however, will be to shift the zeropoint of the relation towards brighter magnitudes and to decrease the apparent slope.

The first three columns of Figure 1 show the distribution of disk scale length R_d, circular velocity ΔV_{circ} calculated from the terminal behavior of the Hα rotation curves, and total *I*-band magnitude $M_I - 5$ log h across the dynamical sample. We have chosen to separate the galaxies into five bins as a function of redshift rather than working on a cluster by cluster basis, given that the incompleteness is a function of distance, to increase the number of points within each bin ($\sim$ 50). There is no strong trend with R_d or with circular velocity, as expected given that our selection technique was not tuned to these variables, and we elect to make no corrections on them. We do expect a strong trend with absolute magnitude, given the magnitude dependence of the selection of our survey objects, and indeed a bias towards increasingly bright intrinsic magnitude shows up clearly as a function of redshift.

The correction for magnitude is made as follows, in the form of previous studies (Giovanelli *et al.* 1997b, Dale *et al.* 1999b). We select a reference frame at rest with respect to the CMB, and apply a type-dependent correction to bring all morphological groups to the same zeropoint (–0.32 magnitudes for Sa and Sab galaxies, –0.10 magnitudes for Sb galaxies). We then model the completeness in absolute magnitude within each redshift bin as a smoothed step function varying between 0 and 1, with the form

$$c(y) = \frac{1}{e^{(y-y_t)/\eta} + 1}, \tag{1}$$

where y_t is a transitional luminosity, decreasing monotonically with bin redshift, and η controls the rate of decay of the function. Having fit $c(y)$ to each bin (see column 4 of Fig-

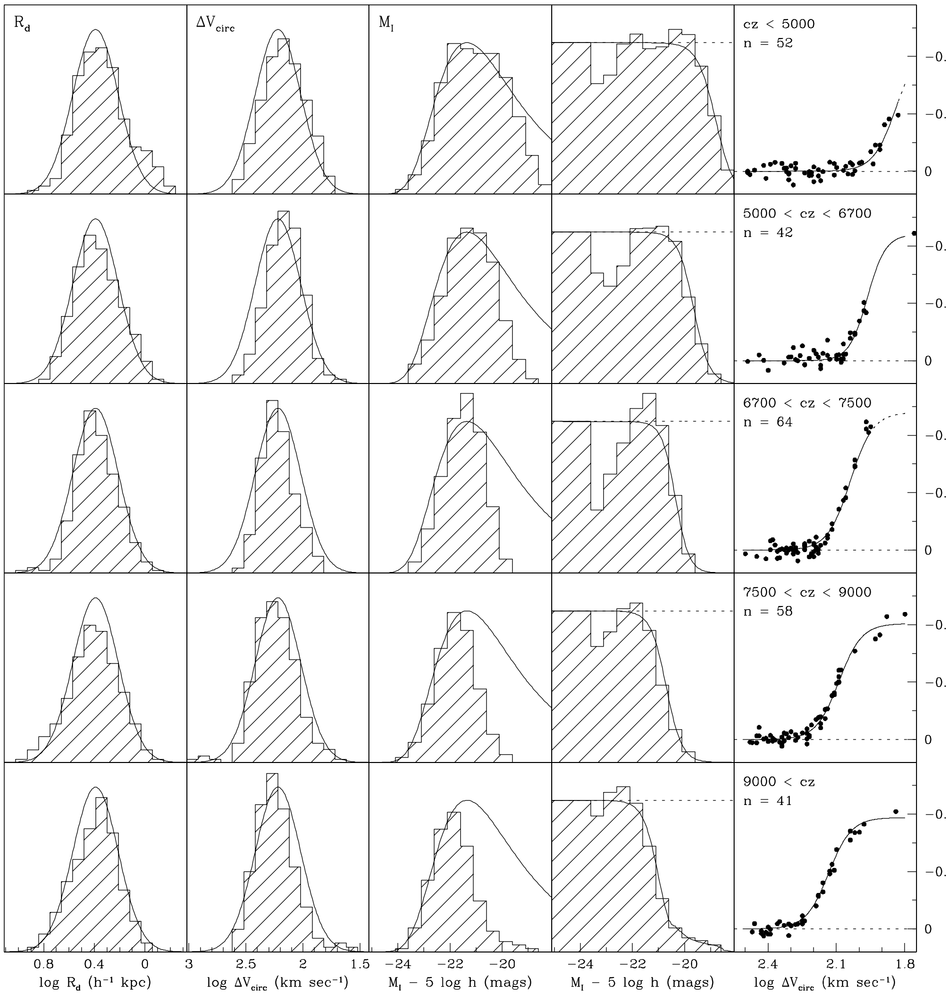

FIG. 1.— Exploration of selection biases throughout the sample, as a function of redshift. The first three columns show the distribution of the sample in size, circular velocity, and luminosity, broken into five redshift bands. A Gaussian function is fit to the size and velocity functions, and frozen across the redshift bins. A Schechter luminosity function (M*=-22.1, α=-0.50) is similarly applied to the magnitude histogram. The fourth column shows the completeness in magnitude varying between 1 (dotted line) and zero. The fifth column shows the incompleteness bias in magnitude for each redshift bin, calculated as discussed in the text, for each galaxy and in a smoothed functional form.

ure 1), we can now evaluate the probable completeness of the sample for each member as a function of velocity width and redshift. For each galaxy, we compute a series of trial magnitudes by assuming the underlying distribution corresponds to the template form of the Tully-Fisher relation (Giovanelli *et al.* 1997b). In each trial,

$$y_{trial} = b_{TF}(\Delta V_{circ} - 2.2) + a_{TF} + f_G\ \Delta_x, \tag{2}$$

where $a_{TF} = -21.01$, $b_{TF} = -7.68$, an offset based on the template scatter $\Delta_x = -0.28(\Delta V_{circ} - 2.2) + 0.26$, and f_G is drawn from a Gaussian distribution with zero mean and unit variance. The value of y_{trial} is stored if the value of $c(y_{trial})$ for the appropriate redshift bin is greater than a random number drawn from the range [0,1]. This process is repeated until 1000 values of y_{trial} have been successfully stored. The incompleteness bias for this object is then computed as the difference between the mean value of y_{trial} and the value expected from the template relation,

$$-\Delta y_{icb} = 0.001 \times \sum_{i=1}^{1000} y_{trial,i} - \{b_{TF}(\Delta V_{circ} - 2.2) + a_{TF}\}\,. \tag{3}$$

A smooth step function function $f_{icb}(\Delta V_{circ})$ is then fit to the distribution of y_{icb} within each redshift bin, as shown in column 5 of Figure 1. As expected, for a given velocity width the incompleteness bias in magnitude decreases from zero with redshift. The functional form of $f_{icb}(\Delta V_{circ})$ is now subtracted from the galaxy magnitudes to counteract the tendency to select brighter objects at a given circular velocity. The maximum bias term is −0.1 magnitudes for our sample, due to the depth of the cluster sampling and the limited range in redshift (cz < 13,000 km s^{-1}).

The next step in comparing fundamental parameters is to compute the corrections for the members of each cluster due to peculiar velocities. Most of the cluster within the dynamical study were examined within Giovanelli *et al.* 1998, and A2151 was examined in Dale *et al.* 1999b, and the peculiar velocities computed therein can be used for this purpose. We proceed to calculate peculiar velocity corrections for the remaining clusters A426 and A539, in the same fashion. For each cluster, we calculate the mean of the error-weighted offsets in magnitude from the template relation for the individual galaxies which are members of the cluster. This gives us values of 0.150 magnitudes (-364 km s^{-1}) for A426 and 0.070

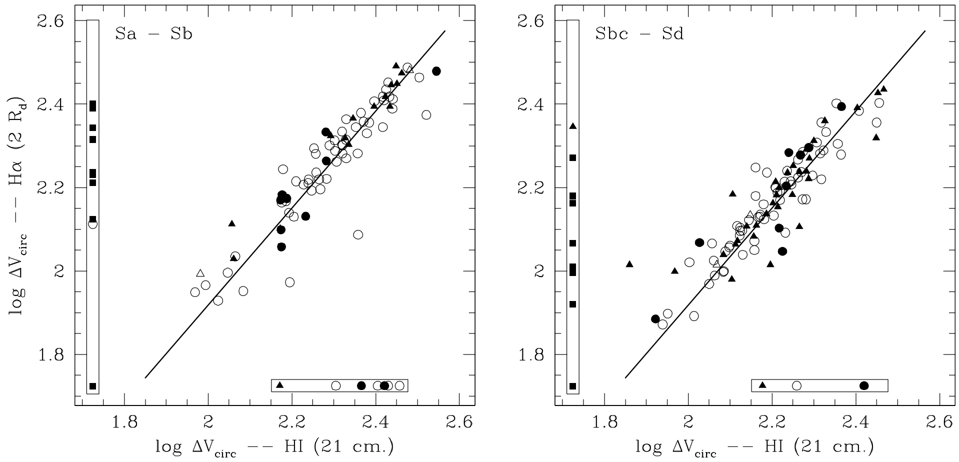

FIG. 2.— Circular velocities of early **(left)** and late **(right)** type spirals derived from H I line profiles and from the Hα emission line flux at 2R$_d$ for H I normal field galaxies (filled triangles), the few H I deficient field galaxies (open triangles), H I normal cluster members (open circles), H I deficient cluster members (filled circles), and H I non-detections (filled squares). The 27 H I non-detections are boxed on the left, and the nine galaxies for which the Hα flux does not extend to 2R$_d$ are boxed below. We find ΔV_{circ} (Hα) = (1.16 $\pm$ 0.03) $\times$ ΔV_{circ} (H I) – (0.049 $\pm$ 0.003).

magnitudes (-277 km s^{-1}) for A539.

2.2. *Parameterizing Velocity Profiles*

We begin by examining the velocity profiles of the galaxies. We have two independent forms of velocity width measurement: the frequency distribution of H I gas, from single-dish H I line profiles, and the spatial and frequency distribution of Hα and [N II] line flux. Because the bulk of H I gas is found at large radii, the H I line profile serves as a good measure of terminal velocity. Hα and [N II] rotation curves are similarly useful, because they typically extend for three to five disk scale lengths, to the outer portion of the optical disk where the velocity profile becomes fairly flat.

Optical rotation curves can be characterized by a steeply sloped inner region (r $\sim\leq$ 1 R$_d$), a transition or elbow point, and then a shallow slope which gradually tapers off to become flat at large (r $\sim$ 4 R$_d$) radii. A clear mechanism for creating rising terminal profiles is to truncate the Hα flux before the profile has leveled off. As discussed in Paper II, such a truncation occurs in spiral galaxies interacting with hot intracluster gas, and is certainly a function of the cluster environment. We have explored previously the good agreement found between velocity widths derived from the terminal, or near-terminal, behavior of optical rotation curves and from H I line profiles (Vogt 1995, Giovanelli *et al.* 1997a, Dale *et al.* 1998). These measurements depend strongly upon the extent of the rotation curve, often requiring a minimum extent to the isophote containing 83% of the *I*-band flux (as proposed by Persic & Salucci 1991, 1995), and containing a correction term dependent upon the steepness of the terminal slope of the rotation curve. This corrective term serves well for peculiar velocity studies, by allowing calculations of cluster positions to be enhanced by the inclusion of spiral galaxies well within the cluster cores (typically H I deficient and with truncated Hα). However, this assumes that the slope-dependent correction term, in effect an extrapolation of the rotation curve behavior beyond its terminal radii, can be applied universally.

In order to evaluate type-dependent factors we divide our sample into early (Sa through Sb) and late (Sbc through Sd) types, and allow the zeropoint for each relation to shift between the two type groups. We elect to measure the disk circular velocity at a smaller radius of 2 R$_d$ throughout the dynamical sample, a distance to which all but nine of the Hα rotation curves extend, and to apply no slope-dependent correction term. Six of the nine have *normal* Hα extent, being fairly large galaxies for which R$_d$ $\sim$ 5 h^{-1} kpc, and the others are *stripped* or *asymmetric*. We note the work of Willick (1999), who found a reduced scatter in the Tully-Fisher relationship of the LP10k catalog by measuring velocity widths at 2.1 R$_d$, in support of the use of V(2R$_d$) in evaluating mass-to-light ratios. This width is equal to the Hα terminal velocity width in many cases; lower values are typically found for slow rising profiles of small or late type spirals which have not reached their full velocity width at 2 R$_d$. The most significant difference within the sample in the percentage rise at 2 R$_d$ lies between early and late type spirals, and we account for this by examining each morphological group separately and in combination.

For *quenched* galaxies, the Hα absorption trough is deep and can be traced through the nucleus and along the major axis. It extends to a radius at or beyond 2 R$_d$ in all but three cases. This makes it possible to determine a velocity width from the optical spectrum as is done for emission line flux, with appropriate corrections between stellar and gas velocities (see discussion in Paper I, also Neistein, Maoz, Rix, & Tonry, 1999). In the few cases where a velocity width can also be measured from the H I data, it is found to be in good agreement with that taken from the Hα absorption line flux.

2.3. *Overview of Fundamental Parameter Relations*

We find that the galaxies observed in the general vicinity of the clusters but more than 3 h^{-1} Mpc from the center have characteristics similar to those of the isolated field spirals, and combine the two populations to form a single population representative of the field. The region more than 3 h^{-1} Mpc from the clusters is typically fairly empty, the exception being that around the A1656 cluster which shows an over-density of spirals at large radii in a bridge extending towards A1367 (see Figure 1 in Paper II). We conducted our analysis with and without the extended spiral population around A1656, and found no significant differences. The three H I deficient field spirals on our sample were not used in fits to the field population; we note that they follow the characteristics of the H I normal field population more than the H I deficient cluster population.

We examined the three relations by dividing our sample galaxies into various subsets. All galaxies within 3 h^{-1} Mpc of the cluster cores which were not background or foreground superpositions were treated as cluster members, including both accreted spirals and infalling subgroups. We inspected each individual cluster in turn, divided the clusters into X-ray hot and X-ray cold groups, and binned galaxies according to their individual H I deficiency. The four clusters with X-ray temperatures greater than 4 keV (A1656, A426, A2199 and A1367) made up the X-ray hot group, and the other clusters and groups were all considered to be X-ray cold.

We found that the offsets from the H I normal field galaxies within the sampled clusters correlated most strongly with H I deficiency, and cluster X-ray temperature. There is, of course, a strong overlap between the H I deficiency and X-ray hot cluster membership (*cf.* Magri *et al.* 1988). H I deficient members of X-ray hot clusters showed strong trends and H I normal members of X-ray cold clusters showed the least deviation from the field spiral population, unsurprisingly, but we note that H I normal members of X-ray hot clusters show more (at marginal significance, however) of a deviation from the field population than do H I deficient members of X-ray cold clusters. The most deviant galaxies within the cluster sample were late type members of X-ray hot clusters, so gas deficient that no generally no H I gas had been detected (to limits of $\sim 5 \times 10^8$ $M_\odot$). Figures 3 through 5 illustrate these trends, as discussed below.

2.3.1. *The Size-Velocity Relation*

Figure 3 shows the relation between disk scale length and circular velocity throughout the dynamical sample. (Disks and bulge surface brightness profiles were deconvolved, and both disk scale lengths and velocities were corrected for inclination, as discussed in Paper I.) We present an average of y–on–x and x–on–y error weighted, 3σ-clipped least-squares fits to the 159 galaxy H I normal population, with the centered variables $x = \log \Delta V_{circ} - 2.20$ and $y = \log R_d - 0.38$, and find the relation $\log R_d = (1.59 \pm 0.18) \times \log \Delta V_{circ} - (3.15 \pm 0.01)$ with early/late morphological types lying at ∓ 0.081. (The offset between field and cluster galaxies is negligible for both H I normal type groups.)

We find an offset from the H I normal early type population to the 28 early type H I deficient galaxies of -0.21 ± 0.15 in $\log R_d$. The nine *quenched* galaxies form the extreme edge of this population, falling at -0.35 ± 0.18 in $\log R_d$, well below the H I normal sample. There are substantially fewer H I deficient late type galaxies, and they exhibit more scatter in all three of the planes which we will examine in Figures 3 through 5. The 21 detected late type H I deficient galaxies lie at a similar offset of from the late type H I normal spirals, at -0.13 ± 0.21, and the three late type *quenched* spirals fall at -0.46 ± 0.16.

One advantage of examining the size-velocity relation is that it is independent of the direct effects of changes in surface brightness, and allows us to focus on the more static properties of disk size and velocity (strongly tied to mass). If the *I*-band disk scale length is unaffected by the suppression of star formation in the disk, as predicted, for example, for models of tidal interactions (Gnedin 2003), this implies that the quenched spiral disks formed at a redshift $z \sim 1$. We treat this epoch as an upper limit as we assume (1) that the disk scale lengths are unlikely to have been larger in the past (*i.e.* stars were built up along the disk from the inside-out), (2) that halo or disk truncation would have only shortened the scale lengths), and (3) that galaxies which are still identifiable as spirals are unlikely to have undergone a major merger, and as we are working at near-infrared wavelengths (less affected by the instantaneous star formation rate than *B*-band). This is in reasonable agreement with observations of disks at high redshift (Lilly *et al.* 1998, Vogt 2000, Le Fèvre *et al.* 2000). Though the shift of [O II] 3727Å out of the optical passband makes spectral redshift determinations for star forming galaxies above a redshift $z \sim 1.2$ fairly difficult, deeply imaged fields such as the two Hubble Deep Fields suggest that the virialized field disk population drops off between $z \sim 1$ and 1.5 (Vogt 2000).

2.3.2. *The Surface Brightness Diagram*

Figure 4 shows the surface brightness properties of the sample. The fit to the H I normal galaxies is $\log R_d = (-0.25 \pm 0.03) \times (M_I^{disk} - 5 \log h) - (4.77 \pm 0.01)$, with the fit to the centered variables $x = M_I^{disk} - 5 \log h + 21.2$ and $y = \log R_d - 0.38$ and early/late types lying at ∓ 0.064. The H I normal cluster galaxies again follow the distribution of the field spirals. We have converted de Jong's (1995) *B*-band surface brightness relation for a range of field spirals into *I*-band, for comparative purposes. Assuming an average $B - I = 1.87$, it becomes $\log R_d = -0.20 \times (M_I^{disk} - 5 \log h) - 3.79$, in reasonable agreement.

The *quenched* population is expected to have faded substantially in *I*-band, given its evolutionary track. We apply a brightening factor of 0.70 magnitudes, (1) in line with projected fading from stellar populations, (2) to match the offset in R_d in the R–V relation with that remaining in surface brightness, and (3) to balance the offset of the *quenched* galaxies within the M–V relation, after examining all three fundamental parameter relations. The offset for early type H I deficient galaxies is then -0.14 ± 0.16 in $\log R_d$, and the *quenched* spirals are again additionally offset, at -0.40 ± 0.10. The late type H I deficient galaxies are offset by -0.13 ± 0.11 in R_d, as in the R–V plane, and we place the late type *quenched* galaxies at -0.35 ± 0.07 in R_d. We note that the blue *asymmetric* galaxies are offset 0.50 mag brighter than the red, which supports their placement in a starbursting phase.

2.3.3. *The Tully-Fisher Relation*

Figure 5 shows the Tully-Fisher relation for our data set. We find an H I normal spiral relation in agreement with the literature, in the range of other *I*-band results (*cf.* Pierce & Tully 1992, Giovanelli *et al.* 1997b, Verheijen 2001). Recall that we are using disk rather than total galaxy magnitudes, with mean bulge fractions of $(13 \pm 9)\%$, and velocity widths measured at 2 R_d as our cardinal variables, and so corrections must be made to transfer from one survey to another to compare results. An average of y–on–x and x–on–y, error weighted least-squares fits to the centered variables $x = \Delta V_{circ} - 2.20$ and $y = M_I^{disk} - 5 \log h + 21.2$ yields the relation $M_I^{disk} - 5 \log h = (-6.31 \pm 0.33) \times \log \Delta V_{circ} - (7.26 \pm 0.01)$, with early/late types lying at ± 0.065.

The offset for early type H I deficient galaxies is 0.003 ± 0.42 in $\log M_I^{disk} - 5 \log h$ (shifting the zeropoint to brighter magnitudes), while the *quenched* spirals are offset by -0.10 ± 0.56. The offsets are similarly small for late type spirals, (0.06 ± 0.47, and 0.29 ± 0.46 for the three late type *quenched*

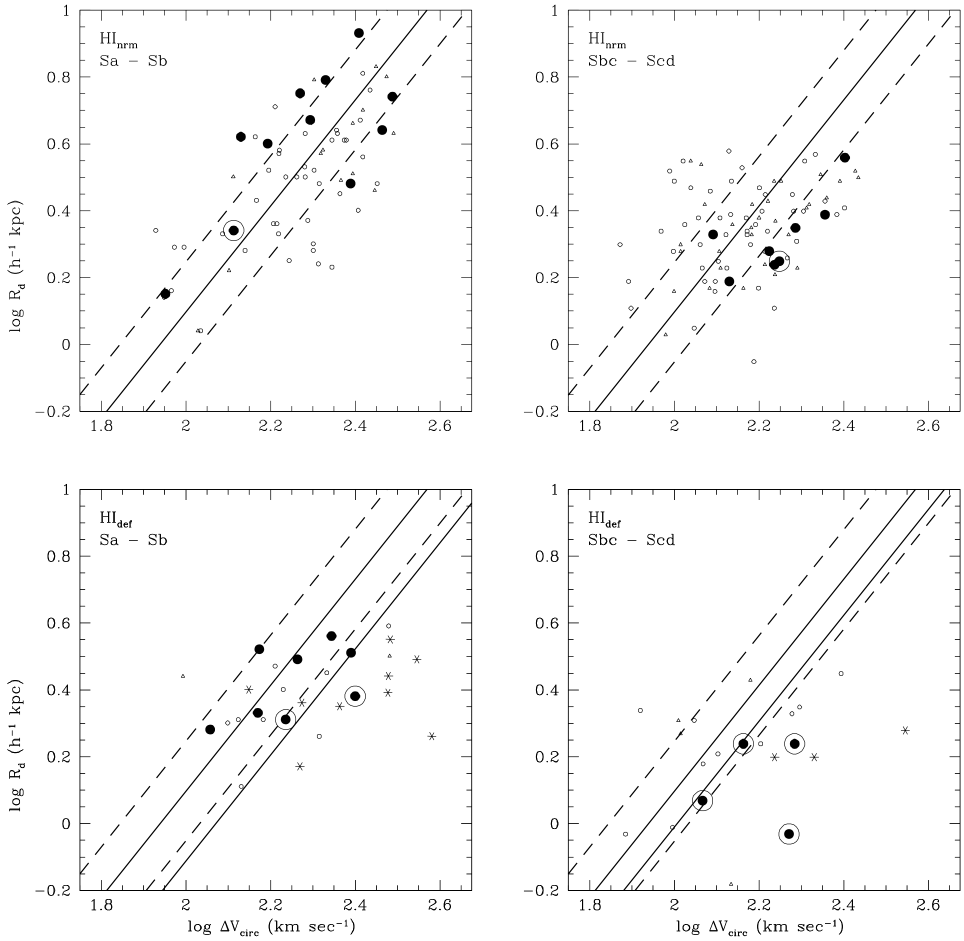

FIG. 3.— Exponential disk scale length R_d as a function of circular velocity ΔV_{circ}, divided into early **(left)** and late **(right)** morphological types, and H I normal **(top)** and H I deficient **(bottom)** spirals. Small open triangles represent isolated field galaxies, and small open circles galaxies within cool clusters or located more than 900 h^{-1} kpc from the core of a warm (kT $>$ 4 keV) cluster. Core members of warm clusters are shown with a large solid circle; those few within the cores of the three hottest clusters (A1656, A426, and A2199) are encircled, and *quenched* galaxies are marked with asterisks. Early and late types were offset by ±0.081 in log R_d to bring the zeropoints of the H I normal morphological groups into agreement, and an error weighted fit to the complete H I normal population, with dashed 1σ limits, is shown in all four windows. The second solid line on the lower plots shows the $\sim$ 30% offset in R_d to the H I deficient galaxies for each morphological group.

spirals). The alignment of the three sub-populations, the H I normal galaxies, and H I deficient, and the *quenched* spirals, in each morphological bin, supports the proposed brightening correction of 0.70 magnitudes for the *quenched* population. If the disk scale lengths of H I deficient galaxies are decremented by $\sim$ 25% as suggested by their distribution in the R−V and the R−M planes, then we may in fact be measuring circular velocities at 1.5 R_d rather than at 2.0 R_d. When we refit these velocity profiles at 2.5 R_d, the offset from the H I normal relation for those that extended that far in Hα became insignificant. As the galaxies for which the extent of Hα is most truncated (between 2.0 and 2.5 R_d) may be those most altered by the stripping process, we re-integrated them into the revised fit by comparing the velocities measured at 2 R_d for the H I deficient population with velocities measured at 1.5 R_d for the H I normal population; again the already small offset became negligible.

In contrast to the R−V and R−M planes, we find that the H I deficient galaxies show no significant offset relative to the H I normal population, with the exception of the *quenched* galaxies. This suggests that, although cluster spirals are smaller than their field counterparts, any alterations to the global brightness or mass either preserve the mass-to-light ratio (moving along the Tully-Fisher relation rather than away from it), or take effect significantly more slowly than the fast ($\Delta t \sim 10^7$ years) H I stripping processes.

Early work with Hα optical rotation curves (Rubin, Whitmore, & Ford 1988; Whitmore, Forbes, & Rubin 1988; Forbes & Whitmore 1989) suggested that the observed velocity profiles declined at large optical radii more in cluster spirals than in the field, implying the presence of substantially stripped or stunted halos, but this result has not been supported by later observations (Distefano *et al.* 1990; Amram *et al.* 1993 two-dimensional velocity maps; Sperandio *et al.* 1995; Vogt 1995; Dale *et al.* 1999a). We have examined the inner and outer slopes of the optical rotation curves calculated by a range of methods, and determined stellar mass-to-light ratios for our sample calculated by a velocity decomposition of the bulge, disk and halo, and find no evidence for significant offsets as a function of H I deficiency or cluster X-ray gas temperature there either. (Note that apparently larger outer slopes of cluster spirals can be accounted for by the radial truncation of the

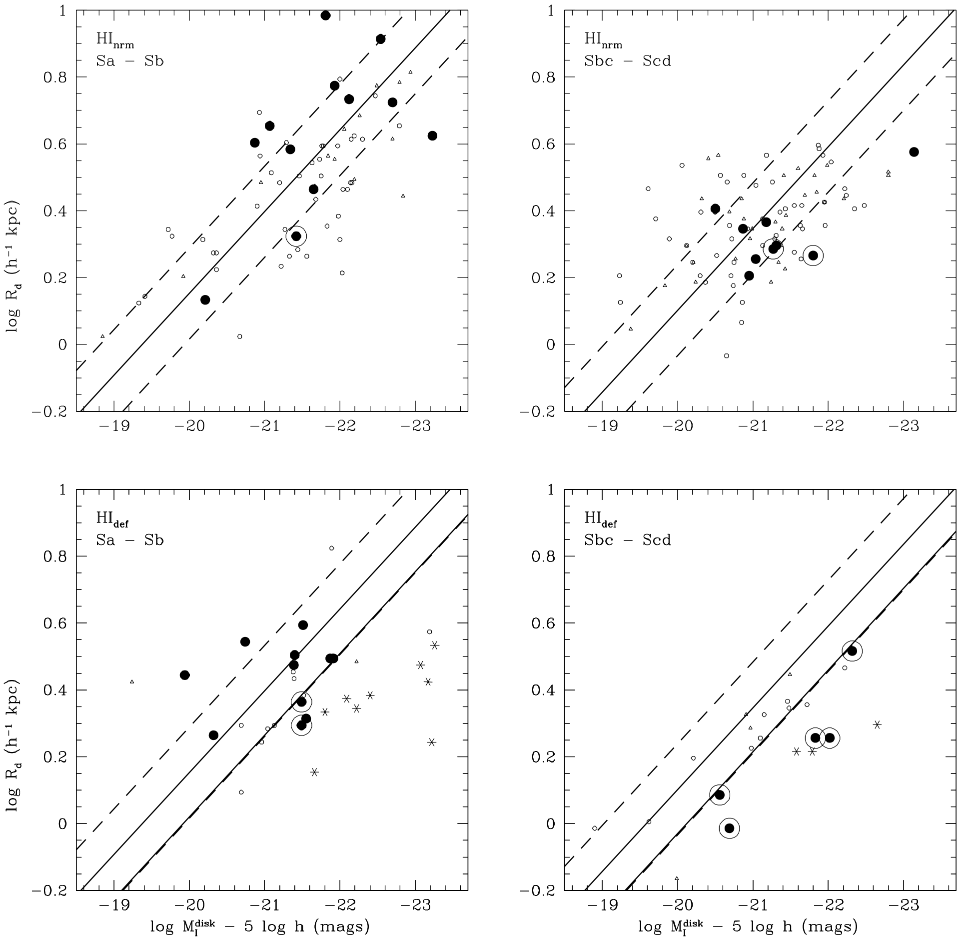

FIG. 4.— Exponential disk scale length R_d as a function of disk *I*-band luminosity $M_I^{disk} - 5$ log h, divided into early **(left)** and late **(right)** morphological types, and H I normal **(top)** and H I deficient **(bottom)** spirals. Symbols are as in Figure 3. Early and late types were offset by ± 0.064 in log R_d to bring the zeropoints of the H I normal morphological groups into agreement, and the *quenched* population was brightened by 0.70 magnitudes. An error weighted fit to the complete H I normal population, with dashed 1σ limits, is shown in all four windows. The second solid line on the lower plots shows the $\sim 25\%$ offset to the H I deficient galaxies for each morphological group.

Hα emission, leading to a measurement biased towards the rising inner part of the curve.) Unfortunately, the Hα velocity profiles of cluster (and of many field) galaxies do not extend to large enough radii for us to constrain the halo core radius or shape significantly. We have performed bulge, disk, and halo fits to the combination of velocity profiles and deconvolved surface brightness profiles (Vogt 1995), but we are unable to provide direct evidence for or against halo truncation within the optical radius.

One could argue, given the lack of change to the full velocity profiles, that the three-plane data shown in Figures 3 through 5 support the case for dark matter domination over baryons in the inner regions of spirals disks. However, we must contrast this with the work of Debattista & Sellwood (2000), who argue that a dominant inner halo would drag down the rotational speed of bars in barred galaxies, and of Dalcanton and of van den Bosch (2000), whose rotation curves of late type, low surface brightness spirals cannot be fit in the cores with any of the standard halo models (*e.g.*, Hernquist, NFW).

The quenched spirals are found to lie 0.70 magnitudes fainter than the H I normal relation, where one would expect a spiral to lie if star formation had previously been halted by removing the gas reservoir without significantly disturbing the stellar structure of the disk (*cf.* Kannappan, Fabricant, & Franx 2002). This is particularly interesting to note, in view of recent work on a Tully-Fisher relation by Hinz, Rix, & Bernstein (2001) and Neistein, Maoz, Rix, & Tonry (1999), finding offsets ≤ 0.2 magnitudes from late type spirals for 18 Coma S0s. In contrast, Magorrian (2000) has used constant-anisotropy spherical dynamical models to study 18 ellipticals and derived an offset ~ 1 magnitude fainter than normal spirals for them. Clearly, morphological type classification (and inclination angles) play an important role in interpreting these results.

In summary, the simplest way to reconcile the offsets shown within the three planes of Figures 3 through 5 is through a decrease in disk scale length of $\sim 25\%$ for H I deficient galaxies, with an additional fading of 0.70 magnitudes for the *quenched* spirals. The *quenched* spirals represent the extreme edge of the truncated population, and the H I normal members of hot cluster cores, though small in number, also follow this trend.

3. STAR FORMATION PROPERTIES

Star formation rates have been studied previously in clusters by use of broadband colors, narrow-band Hα photometry,

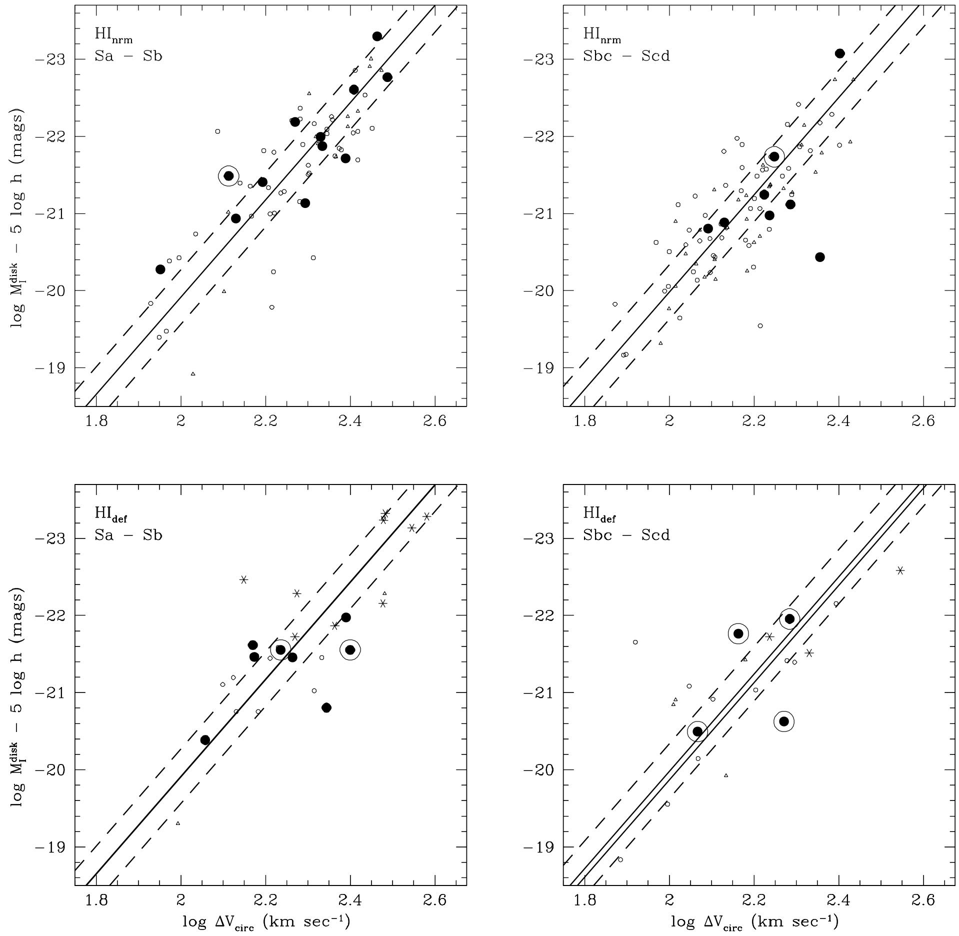

FIG. 5.— Disk I-band luminosity $M_I^{disk} - 5$ log h as a function of circular velocity ΔV_{circ}, divided into early **(left)** and late **(right)** morphological types, and H I normal **(top)** and H I deficient **(bottom)** spirals. Symbols are as in Figure 3. Early and late types were offset by ∓ 0.065 in $M_I^{disk} - 5$ log h to bring the zeropoints of the H I normal morphological groups into agreement, and the *quenched* population was brightened by 0.70 magnitudes. An error weighted fit to the complete H I normal population, with dashed 1σ limits, is shown in all four windows. The second solid line on the lower plots shows the minimal offset to the H I deficient galaxies for each morphological group.

and Hα equivalent widths. Kennicutt *et al.* (1984) observed that many cluster spirals had star formation properties equivalent to those of field spirals and that H I deficiency did not necessarily imply a change in the overall star formation rate. Recent work on circumnuclear starbursts has identified probable tidal-interaction candidates in the cores of rich clusters (Moss & Whittle 2000; see also Andersen 1999) and extensive analyses of the Virgo cluster (Koopmann 1997; Gavazzi *et al.* 2002a, 2002b) has targeted star formation suppression in the outer parts of cluster disks through a variety of H I gas stripping and redistribution mechanisms.

We looked for evidence within the dynamical sample supporting Koopmann's finding that a substantial fraction of cluster spirals are assigned early spiral type Hubble types due to low global star formation rates, though their central light concentrations are more representative of late type spirals (*i.e.* stripped late type spirals are systematically misclassified as early types). Lacking central concentration measurements, we examined I-band bulge-to-total (B/T) fractions as a function of galaxy type, but found no significant trend with H I deficiency. We do not find evidence for H I deficient, late type interlopers, with small bulge fractions, within the early type classifications. However, we do note that the *asymmetric* late type galaxies have larger B/T fractions and redder $B-I$ colors than *normal* late type spirals, suggesting a shift toward certain early type qualities. There is an offset of ± 0.075 in log R_d between late and early morphological type galaxies regardless of H I gas content (Figures 3 and 4). Because of this, stripped late type galaxies classified as early types could contribute to the smaller offset observed for H I deficient early type galaxies than for late types, as they would fall closer to the H I normal early type galaxy relation than to that for late types.

We lack Hα photometry and multi-band aperture colors for our sample, but the distribution and extent of Hα along the $1''$slits we placed along the galaxy major axes provides a tracer of young star formation. Figure 10 in Paper II shows the distribution of Hα_{ext} emission throughout the dynamical sample. Hα_{ext} is shown as a function of R_d, thus taking into account the decrement of 25% in R_d found for the H I deficient galaxies. An average of y–on–x and x–on–y, error weighted least-squares fits, conducted on the centered variables x = log R_d − 0.38 and y = log Hα_{ext} − 0.90, yields the one-to-one relation log Hα_{ext} = (0.85 ± 0.06) × log R_d + (0.62 ± 0.09) for H I normal galaxies, with no significant offset (∓ 0.01 in log Hα_{ext}) between morphological types. The early type H I deficient spirals have truncated emission for their size, by −0.13 ±

0.07 in log $H\alpha_{ext}$ (equivalent to a decrease of 26% in $H\alpha_{ext}$). In contrast, the H I emission in the H I deficient late type spirals shows no significant change in length (–0.01 ± 0.09). If $H\alpha_{ext}$ was unchanged by the stripping process and by the cause of the change in R_d, we would expect an apparent offset of +0.12, due to the decrement of 25% in log R_d in H I deficient galaxies. The observed decrement of R_d, isolated in the plots of fundamental parameters for spirals of *all morphological types*, is not echoed in Hα truncation, which suggests that the change in R_d is not an artifact of the H I stripping process. The extent of the Hα absorption trough along the major axes of the *quenched* spirals is significantly more truncated than the distribution of the Hα emission line for H I deficient galaxies. The distribution of the old stellar population contributing to the $H\alpha_{ext}$ absorption of the *quenched* spirals may be partly responsible for this extreme truncation, if disks are built up from the inside to the outside over time.

A contrasting result from a recent large-scale study of 510 rotation curves (Dale *et al.* 2001) found weaker trends in the extent and asymmetry of the Hα flux with clustercentric radius. The strong selection bias of the survey towards galaxies with strong, extended Hα or [N II] 6584Å emission, chosen by eye to lack a dominant bulge component (Dale *et al.* 1997), and of late type (70% are Sbc or later, Sc galaxies alone make up 52%, Dale *et al.* 1999a) in effect has biased the sample against the galaxies which show the most change in Hα, and explains our contrasting results.

We note that the combined effects of disk size decrement and $H\alpha_{ext}$ truncation can also well explain the apparent increase in rotation curve outer slopes for certain cluster spirals reported in Vogt (1995). By truncating the Hα flux within the inner regions of the rotation curve, before the curve has leveled off to a terminal straight relation, and decrementing R_d, one can measure an inflated, high slope by fitting the *decremented* final extent of the rotation curve at smaller radii.

If the changes in R_d are due to the galaxies within in the rich cluster cores having formed at an early epoch, the truncation of $H\alpha_{ext}$ is best attributed to the direct effects of the galaxy local environment, be it H I gas stripping through interaction with the intracluster medium, galaxy harassment or tidal effects. This is supported by the distribution of the *asymmetric* spirals through the plot. The H I deficient *asymmetric* spirals follow the relation of the general H I deficient spirals. Those which are still fairly gas-rich, however, and thus assumed have only recently begun the stripping process, show an interesting feature. When $H\alpha_{ext}$ is defined as the *shorter* extent of Hα along either side of the disk, the gas-rich asymmetric spirals follow the relation of the general H I deficient spirals. When we examine the *longer* extent of Hα, however, we find that these galaxies follow the relation of H I normal spirals. This implies, in support of Koopmann 1997, that the complete stripping process is systematically truncating star formation in the outer parts of the disk.

Figure 6 shows similarly that the *B*-band radii R_b are smaller in the H I deficient early type galaxies than in the H I normal sample; as with the Hα extent, we do not see an equivalent drop in the late type galaxies. We find log R_b = (0.89 ± 0.06) × log R_d + (0.71e± 0.08) for H I normal galaxies, with no significant offset (∓0.01 in log R_b) between morphological types. The early type H I deficient cluster spirals are offset from the H I normal field population by 0.02 ± 0.09 in log R_b. (There is a small offset to the *quenched* population, at 0.05 ± 0.10.) If R_b was unchanged by the stripping process, we would expect an offset of 0.11, caused by the decrement of 25% in log R_d in H I deficient galaxies. The late type H I deficient cluster spirals are offset from the H I normal population by 0.08 ± 0.10, suggesting that R_b is unchanged by the stripping process for recognizably late type spirals. The scatter in the $R_b - R_d$ relationship is large, but this suggests that R_b, like $H\alpha_{ext}$, is decremented in the stripping process, while the decrement in the R_d may be a remnant of an early formation epoch. Assuming a constant young star formation rate, it is possible that a formation-era initial decrement in R_b could be subsumed within later star formation and radially increasing disk growth.

Figure 7 shows the distribution of H I gas content across the dynamic sample as a function of R_b and morphological type, the two variables commonly used in modeling expected gas masses (*cf.* Solanes, Giovanelli, & Haynes 1996 and references therein). The distribution of H I mass is fairly continuous; there is no zone of avoidance between normal and deficient states. Almost none of the galaxies for which we have an upper limit on the gas content lie above the zone of substantial (40%) H I deficiency. The difference in the predicted amount of H I gas as a function of morphological type is far less than the distinction between the H I normal and H I deficient categories. However, due to the steep slope of the relation for late type spirals, if any of the H I deficient galaxies classified as early type are late type spirals which have undergone a partial morphological transformation, the degree of H I gas mass loss could be under/over-estimated by up to a factor of two for large/small values of R_d. We note also that the decrement in R_b observed for early type, H I deficient galaxies (Figure 6) would translate into an underestimate of H I gas deficiency of 20% for these galaxies.

4. CONCLUSIONS

We have conducted a study of optical and H I properties of spiral galaxies to explore the role of gas stripping as a driver of morphological evolution in clusters. For H I deficient local cluster spirals (with less than 40% of the predicted atomic gas mass), we observe a decrease of a factor of 25% in *I*-band disk scale lengths relative to H I normal spirals in spirals of all morphological types. This may be a relic of early galaxy formation, caused by the disk coalescing out of a smaller, denser halo (*e.g.*, higher concentration index) or reflect an environmental effect (*e.g.*, truncation of the hot gas reservoir at large radius due to the high local density of neighboring galaxies), or it may be be the product of post disk-formation effects (*e.g.*, gas stripping, tidal interactions). The few H I normal spirals observed in the cores of rich clusters are similarly decremented, in support of the former.

B-band radii R_b are decreased by 25% relative to H I normal field galaxies in H I deficient early type spirals (Sa through Sb). They show an additional decrease of 55% in the extent of the Hα flux along the disk, on or within the stripping radius predicted for the H I gas loss from models. Gas-rich *asymmetric* spirals reflect this trend on the truncated side of the disk, implying that it is caused by the gas stripping process. Late type spirals (Sbc through Scd) exhibit neither trend, suggesting that either gas removal is less effective within the potential or that once significant star formation suppression occurs these galaxies are no longer identified as late type spirals.

For star forming spiral galaxies associated with all of the clusters, we find no significant trend in stellar mass-to-light ratios or circular velocities with H I gas content, morphologi-

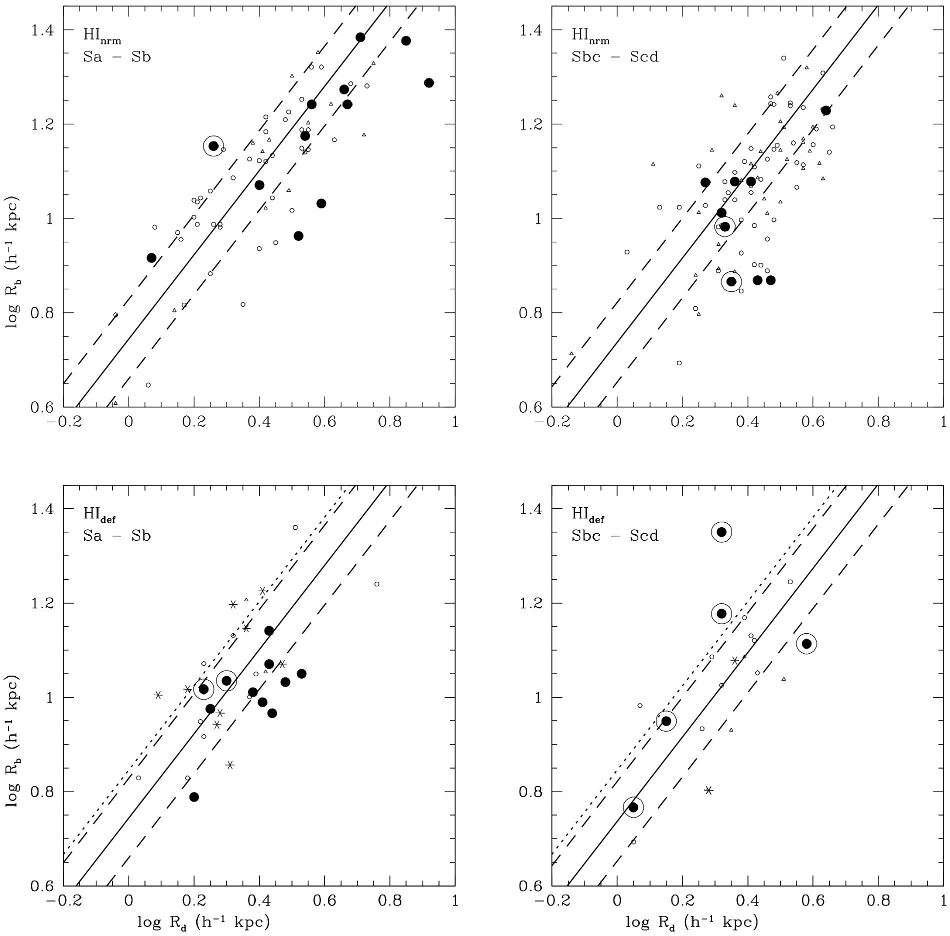

FIG. 6.— B-band radius R_b as a function of exponential disk scale length R_d, divided into early **(left)** and late **(right)** types, and H I normal **(top)** and H I deficient **(bottom)** spirals. Symbols are as in Figure 3. An error weighted fit to the H I normal population is shown on the top two plots, with 1σ limits, and reproduced on the bottom two plots. The second line (dotted) on the lower plots designates the predicted relation *if* R_d was decremented by 25% for H I deficient galaxies, but R_b remained unchanged; the distribution of early type H I deficient galaxies is in clear disagreement.

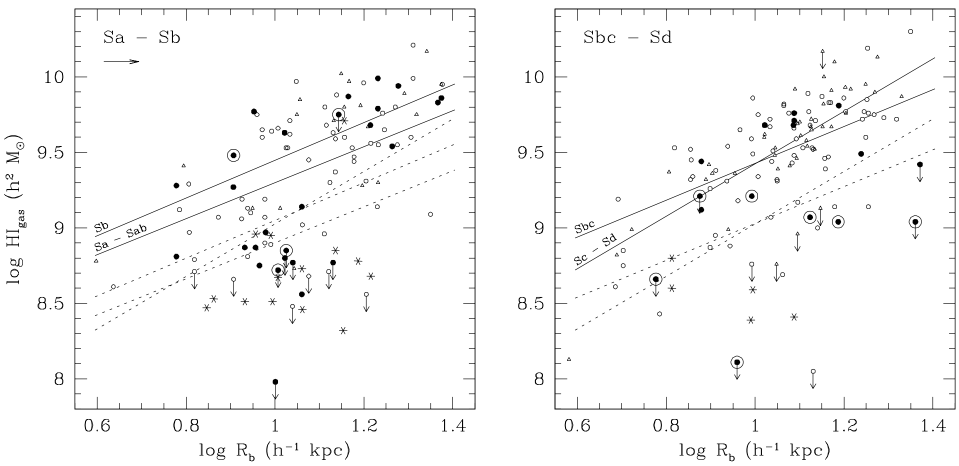

FIG. 7.— The total H I gas mass vs. blue radius R_b for early (**left**) and late type (**right**) galaxies. Symbols are as in Figure 3. Upper limits are drawn for all undetected galaxies, with the exception of the *quenched* population (hidden there to simplify the plots, as all but two are undetected). The solid lines show the normal relations used to calculate H I deficiency as a function of R_b for various galaxy types, and the dashed lines below the H I gas upper limit for the H I deficient population (less than 40% of the expected gas mass) for each type. The relations for Sb (left) and Sbc (right) fall virtually on top of each other; the relation for earlier type (left) galaxies lies at 70% of the Sb line, while the relation for later types has a much stronger dependence on R_b. The H I deficiency limit for late (Sbc through Scd) types has been reproduced on the lefthand plot. The arrow in the upper lefthand corner shows the decrement in R_b that the early type H I deficient galaxies may have endured in the process of being stripped, which could lead to an underestimate of 20% in the H I gas loss.

cal type, or clustercentric radius. This could be interpreted as support for dark matter domination over baryons well within the optical radius of disks.

In summary, we have explored the formation and evolution of spiral galaxies in local clusters through a combination of optical and H I properties. We find evidence that the spirals within rich cluster cores, believed to coalesce from their halos at an early epoch, formed with intrinsically smaller disks than the local field population. We have explored the relationship between H I gas stripping and the consequential suppression of young star formation in spiral galaxies. We find that the ram pressure stripping and the suppression of star formation both occur quickly within spirals infalling into an intracluster medium of hot gas, but find little evidence for substantial mass stripping beyond that of the H I gas.

5. ACKNOWLEDGMENTS

The data presented in this paper are based upon observations carried out at the Arecibo Observatory, which is part of the National Astronomy and Ionosphere Center (NAIC), at Green Bank, which is part of the National Radio Astronomy Observatory (NRAO), at the Kitt Peak National Observatory (KPNO), the Palomar Observatory (PO), and the Michigan–Dartmouth–MIT Observatory (MDM). NAIC is operated by Cornell University, NRAO by Associated Universities, inc., KPNO and CTIO by Associated Universities for Research in Astronomy, all under cooperative agreements with the National Science Foundation. The MDM Observatory is jointly operated by the University of Michigan, Dartmouth College and the Massachusetts Institute of Technology on Kitt Peak mountain, Arizona. The Hale telescope at the PO is operated by the California Institute of Technology under a cooperative agreement with Cornell University and the Jet Propulsion Laboratory. We thank the staff members at these observatories who so tirelessly dedicated their time to insure the success of these observations. We also thank Sc project team members John Salzer, Gary Wegner, Wolfram Freudling, Luiz da Costa, and Pierre Chamaraux, and also Shoko Sakai and Marco Scodeggio, for sharing their data in advance of publication. The text of this manuscript was much improved by careful reading on the part of Richard Ellis. We thank the anonymous referee for helpful comments on the manuscript.

N.P.V. is a Guest User, Canadian Astronomy Data Center, which is operated by the Dominion Astrophysical Observatory for the National Research Council of Canada's Herzberg Institute of Astrophysics. This research has made use of the NASA/IPAC Extragalactic Database (NED) which is operated by the Jet Propulsion Laboratory, California Institute of Technology, under contract with NASA, and NASA's Astrophysics Data System Abstract Service (ADS). This research was supported by NSF grants AST92–18038 and AST95–28860 to M.P.H. and T.H., AST90–23450 to M.P.H., AST94–20505 to R.G., and NSF–0123690 via the ADVANCE Institutional Transformation Program at NMSU, and NASA grants GO-07883.01-96A to N.P.V. and NAS5–1661 to the WFPC1 IDT. N.P.V. acknowledges the generous support of an Institute of Astronomy rolling grant from PPARC, reference number PPA/G/O/1997/00793.

REFERENCES

Aaronson, M., Bothun, G. D., Mould, J., Huchra, J. P., Schommer, R. A., & Cornell, M. E. 1986, ApJ, 302, 536
Amram, P., Sullivan, W. T., III, Balkowski, C., Marcelin, M., & Cayatte, V. 1993, ApJ, 403, L59
Andersen, V. E. 1999, Ph.D. thesis, University of Alabama
Biviano, A., *et al.* 1990, ApJS, 74, 325
Cole, S., Aragon-Salamanca, A., Frenk, C. S., Navarro, J. F., & Zepf, S. E. 1994, MNRAS, 271, 781
Dalcanton J. J., Spergel, D. N., & Summers, F. J. 1997, ApJ, 482, 659
Dale, D. A., Giovanelli, R., Haynes, M. P., Hardy, E., & Campusano, L. E. 1999b, AJ, 118, 1468
Dale, D. A., Giovanelli, R., Haynes, M. P., Campusano, L. E., & Hardy, E. 1999a, AJ, 118, 1489
Dale, D. A., Giovanelli, R., Haynes, M. P., Hardy, E., & Campusano, L. E. 2001, AJ, 121, 1886
Dale, D. A., Giovanelli, R., Haynes, M. P., Scodeggio, M., Hardy, E., & Campusano, L. E. 1997, AJ, 114, 455
Dale, D. A., Giovanelli, R., Haynes, M. P., Scodeggio, M., Hardy, E., & Campusano, L. E. 1998, AJ, 115, 418
Debattista, V. P., & Sellwood, J. A. 2000, ApJ, 543, 704
de Jong, R. S. 1995, Ph.D. thesis, University of Groningen
Distefano, A., Rampazzo, R., Chincarini, G. L., & de Souza, R. 1990, A&AS, 86, 7
Forbes, D. A., & Whitmore, B. C. 1989, ApJ, 339, 657
Gavazzi, G., Bonfanti, C., Sanvito, G., and Boselli, A., & Scodeggio, M. 2002a, ApJ, 576, 135
Gavazzi, G., Boselli, A., Pedotti, P., Gallazzi, A., & Carrasco, L. 2002b, A&A, 396, 449
Giovanelli, R., Haynes, M. P., Herter, T., Vogt, N. P., Wegner, G., Salzer, J. J., da Costa, L. N., & Freudling, W. 1997a, AJ, 113, 22
Giovanelli, R., Haynes, M. P., Herter, T., Vogt, N. P., Wegner, G., Salzer, J. J., da Costa, L. N., & Freudling, W. 1997b, AJ, 113, 53
Giovanelli, R., Haynes, M. P., Salzer, J. J., Wegner, G., da Costa, L. N., & Freudling, W. 1998, AJ, 116, 2632
Gnedin, O. Y. 2003, ApJ, 582, 141
Guzmán, R. 1993, Ph.D. thesis, University of Durham
Hinz, J. L., Rix, H., & Bernstein, G. M. 2001, AJ, 121, 683
Jablonka, J., & Arimoto, N. 1992, A&A, 255, 63
Kannappan, S. J., Fabricant, D. G., & Franx, M. 2002, AJ, 123, 2358
Kauffmann, G. 1995, MNRAS, 274, 153
Kauffmann, G., White, S. D. M., & Guiderdoni, B. 1993, MNRAS, 264, 201
Kennicutt, R. C., Jr., Bothun, G. D., & Schommer, R. A. 1984, AJ, 89, 1279
Koopmann, R. A. 1997, Ph.D. thesis, Yale University
Le Fèvre, O., *et al.* 2000, MNRAS, 311, 565
Lilly, S., *et al.* 1998, ApJ, 500, 75
Lucey, J. R., Gray, P. M., Carter, D., & Terlevich, R. J. 1991, MNRAS, 248, 804
Lynden-Bell, D., Faber, S. M., Burstein, D., Davies, R. L., Dressler, A., Terlevich, R. J., & Wegner, G. 1988, ApJ, 326, 19
Magorrian, S. J. 2000, in ASP Conf. Ser. 197, XV^{th} IAP Meeting Dynamics of Galaxies: From the Early Universe to the Present, ed. F. Combes, G. A. Mamom, & V. Charmandaris (San Francisco: ASP), 205
Magri, C., Haynes, M. P., Forman, W., Jones, C., & Giovanelli, R. 1988, ApJ, 333, 136
McGaugh, S. S. 2000, in ASP Conf. Ser. 197, XV^{th} IAP Meeting Dynamics of Galaxies: From the Early Universe to the Present, ed. F. Combes, G. A. Mamom, & V. Charmandaris (San Francisco: ASP), 153
Mo, H. J., Mao, S., & White, S. D. M. 1998, MNRAS, 295, 319
Moss, C., & Whittle, M. 2000, MNRAS, 317, 667
Neistein, E., Maoz, D., Rix, H.-W., & Tonry, J. L. 1999, AJ, 117, 2666
Persic, M. & Salucci, P. 1991, ApJ, 368, 60
Persic, M. & Salucci, P. 1995, ApJS, 99, 501
Pierce, M. J., & Tully, R. B. 1992, ApJ, 387, 47
Rhee, M.-H. 1996, Ph.D. thesis, University of Groningen
Rubin, V. C., Whitmore, B. C., & Ford, W. K. 1988, ApJ, 333, 522
Salucci, P., Frenck, C. S., & Persic, M. 1993, MNRAS, 262, 392
Scodeggio, M., Solanes, J. M., Giovanelli, R., & Haynes, M. P. 1995, ApJ, 444, 41
Solanes, J. M., Giovanelli, R., & haynes, M. P. 1996, ApJ, 461, 609
Sperandio, M., Chincarini, G., Rampazzo, R., & de Souza, R. 1995, A&AS, 110, 279
Tóth, G., & Ostriker, J. P. 1992, ApJ, 389, 5
Tully, R. B., & Fisher R. 1977, A&A, 54, 661
van den Bosch, F. C. 2000, ApJ, 530, 177
Verheijen, M. A. W. 2001, ApJ, 563, 694
Vogt, N. P. 1995, Ph.D. thesis, Cornell University
Vogt, N. P. 2000, in ASP Conf. Ser. 193, The Hy-Redshift Universe: Galaxy Formation and Evolution at High Redshift, ed. A. J. Bunker & W. J. M. van Breugel (San Francisco: ASP), 145

Vogt, N. P., Haynes, M. P., Herter, T., & Giovanelli, R. 2004a, ApJ, in press (Paper I)
Vogt, N. P., Haynes, M. P., Giovanelli, R., & Herter, T. 2004b, ApJ, in press (Paper II)
Vogt, N. P., Faber, S. M., Koo, D. C., Phillips, A. C. *et al.* 2004c, in preparation
Whitmore, B. C., Forbes, D. A., & Rubin, V. C. 1988, ApJ, 333, 542
Willick, J. A. 1999, ApJ, 516, 47